CHAPTER 297

An Analysis of Particle Saltation Dynamics

Michael R. Krecic[1] and Daniel M. Hanes[2]

Abstract

A two-dimensional particle saltation model for unidirectional flow is applied to simulate the motion of single particles. The equations of motion include added mass, gravity, drag, shear lift, Basset history, and Magnus or spin lift forces. A sensitivity analysis is performed on the forces, initial lift-off speeds and angles, and for different size particles. The Magnus lift force is found to have a significant effect on a particle's trajectory for coarse sand sized and larger particles. The shear lift and Basset history forces cause particles to saltate farther. Most of the forces vary with particle size. The model predictions compare favorably to observations if appropriate initial conditions are assumed.

Introduction

The term saltation was first used by Gilbert (1914) and comes from the Latin word "saltare" meaning to leap or dance. Saltation is analogous to a ballistic trajectory in the sense that trajectories are smooth and not strongly influenced by turbulent fluctuations. However, hydrodynamic forces such as lift and drag significantly influence the particles' trajectory (Nino, Garcia, and Ayala, 1992).

Fernandez Luque and van Beek (1976) performed experiments in a flume with different bed slopes. They were able to measure the mean critical bed shear stress for the initiation of motion, rate of bedload transport, average particle velocity, and the average length of individual saltations. This was accomplished through the use of high speed photography. Two different sediment types, gravel and magnetite, were studied. When they compared their model results, they concluded that a lift force was needed to explain the observed saltation characteristics.

[1] Research Assistant, Coastal and Oceanographic Engineering Department, University of Florida, Gainesville, FL 32611

[2] Associate Professor, Coastal and Oceanographic Engineering Department, University of Florida, Gainesville, FL 32611

There is some debate as to what angles the saltating particles leave the bed. Owen (1964) examined particle saltation in air. Owen suggested that those particles that leave the bed nearly vertically with a certain initial speed will saltate to a higher elevation than those with other initial angles. White and Schulz (1977), in contrast, observed that particles in air eject at angles ranging from 30 to 70 degrees.

Other researchers such as Murphy and Hooshiari (1982), van Rijn (1984), Wiberg and Smith (1985), Nino and Garcia (1992), and Lee and Hsu (1994) have tried to derive a set of equations to describe the motion of a particle in saltation from bed ejection to bed impact based on the fluid forces. This paper focuses on developing a complete equation of motion from a Lagrangian perspective and provides a detailed analysis of the model parameters.

Particle Saltation Model

This model simulates the trajectory of a single saltating sphere in a steady state, unidirectional flow. An equation of motion is developed and evaluated using previous experimental observations. Models based on only drag and gravity proved insufficient, so other forces have been included, as will be described below. Some of these other forces are found to be significant while others can be ignored in certain situations. What follows is a brief description of the relevant forces.

The effect of gravity is usually written as a submerged weight,

$$\mathbf{F}_G = (\rho_s - \rho) g V \tag{1}$$

where V is the volume of the particle. Obviously, this force increases with increasing particle size because of its dependence on the volume of a particle.

The added mass force arises from the relative accelerations of the particle and the fluid. A submerged body induces accelerations on a fluid if the body is moving with an acceleration relative to the surrounding fluid. The particle can be thought of as having an 'added mass' of fluid attached to its own mass when it accelerates relative to the surrounding fluid (Patel, 1989). The added mass force is given by Auton et al. (1988) as

$$\mathbf{F}_A = -\rho C_M V \left(\frac{d\mathbf{u}}{dt} - \frac{Du_f}{Dt} \right) \tag{2}$$

where $\mathbf{u}$ is the particle velocity, u_f is the fluid velocity, and C_M is the added mass coefficient. The added mass coefficient is defined as a ratio of the additional mass of fluid that is accelerated with the particle to the mass of the displaced fluid by the particle. For a sphere, C_M equals 0.5.

A drag force is a net force in the direction of the fluid relative to the body due to pressure and viscous forces on the body. The drag force on a particle may be written as

$$\mathbf{F}_D = C_D A \frac{1}{2} \rho \mathbf{V}_r^2 \tag{3}$$

where C_D is the coefficient of drag, A is the cross-sectional area of the particle normal to the force, and $\mathbf{V}_r$ is the relative velocity (Fredsoe and Deigaard, 1992). The drag coefficient is a strong function of Reynolds number and shape; thus, it is generally not constant. There have been many empirical formulas for C_D such as those found by Graf (1984) and Morsi and Alexander (1972) which provide C_D as a function of particle Reynolds number. The following formula is used for this analysis:

$$C_D = \frac{24}{\mathrm{Re}} + \frac{7.3}{1+\sqrt{\mathrm{Re}}} + 0.25 \tag{4}$$

where Re is the Reynolds number, $\mathrm{Re} = \frac{\mathbf{V}_r d}{\nu}$

In shear flow the particle develops a pressure gradient across it which results in a lift force, which is commonly called the shear lift force. This phenomenon can be attributed to the Bernoulli effect where the lift force acts in the direction of the velocity gradient. The shear lift force may be written as

$$F_L(shear) = C_L A \frac{1}{2} \rho \left(u_{\Delta Top}^2 - u_{\Delta Bot}^2 \right) \tag{5}$$

where C_L is the lift coefficient and A is the cross-sectional area of the particle normal to the force. The $u_{\Delta Top}$ and $u_{\Delta Bot}$ are the relative velocities evaluated at the top and bottom of the particle, respectively (Wiberg and Smith, 1985).

The lift coefficient has been related to the drag coefficient by Chepil (1958). He conducted experiments involving evenly-spaced hemispheres and allowed wind to flow over them. He then proceeded to calculate drag, lift, and the ratio of lift to drag for different wind speeds. It was determined that the ratio was approximately equal to 0.85; therefore we assume here that C_L equals 0.85 times C_D.

A. B. Basset (1888) first acknowledged that a particle's history had a role in the present particle path; hence, the Basset history force bears his name. Mei (1995) described the force as

> ... derived from the diffusion of vorticity generated at the surface of the particle at a rate proportional to the particle's relative acceleration. Since the diffusion rate is finite, this means that the force is dependent on the history of the particle motion.

Consider a sphere in a steady fluid and then instantaneously increasing the flow to some higher value. It takes some time for the boundary layer on the sphere to adjust to the new flow intensity. This time is accounted for through the Basset history force. The Basset force is defined as

$$\mathbf{F}_B = 6\rho\sqrt{\pi\nu}\left(\frac{d}{2}\right)^2 \int_0^{t_s} \frac{\frac{d\mathbf{u}}{dt} - \frac{d\mathbf{u}_f}{dt}}{\sqrt{t_s - \tau}} d\tau \tag{6}$$

where $\mathbf{u}_f$ is the fluid velocity, ν is the kinematic viscosity, t_s is time, and τ is a dummy variable (Mei, 1994). This force has both a vertical and horizontal component. For steady, shear flow, the fluid acceleration is zero, so the term can be simplified to be a function of the particle acceleration.

In addition to the shear lift force, the Magnus lift force also results from the velocity gradient across the particle. This force, named for Heinrich Magnus who first discovered the phenomenon in 1853, is a pressure force due to the circulation around a spinning sphere (Murphy and Hooshiari, 1982). As a result of viscous effects, angular momentum is supplied to the particle. This force accounts for the different types of pitches in baseball such as the curveball and the slider (Munson, Young, and Okiishi, 1990). The shear flow induces a rotation which causes a particle to saltate higher and further than without the inclusion of this term. If the velocity gradient is positive, the particle will rotate clockwise (cw); hence, an upward lift. If the velocity gradient is negative, the particle will rotate counterclockwise (ccw); hence, a downward lift. For a moving sphere in a shear flow, the force is expressed as

$$\mathbf{F}_L(Magnus) = \frac{\pi}{8} d^3 \rho V_r \left(\Omega - \frac{1}{2}\frac{d\mathbf{u}_f}{dz}\right) \tag{7}$$

with Ω as the angular velocity of the particle with units in rad/s (White and Schulz, 1977). This force was developed from the work of Rubinow and Keller (1961). Rubinow and Keller (1961) looked at rotating a moving sphere in a still viscous fluid with low Reynolds numbers only. Based on their analysis, the Magnus force was independent of viscosity. From this they derived the form of the Magnus force and the moment acting on the sphere. The force has been described previously. The moment has the form

$$Moment = I\frac{d\Omega}{dt} = -\pi\mu d^3\left(\Omega - \frac{1}{2}\frac{d\mathbf{u}_f}{dz}\right) \tag{8}$$

where I is the particle's moment of inertia. This moment equation is solved simultaneously with the equations of motion to constantly adjust the particle rotation to that induced by the fluid. Note that the dynamic viscosity appears in (8). It acts to dampen the effects of the initial particle rotation to that of the fluid. It must be said that the Magnus force and moment equations were derived for small Reynolds numbers. We consider the Magnus force in this shear flow analysis for the purpose of determining whether the effect improves the agreement between experiments and theory.

Applicability of Forces For Different Reynolds Number Ranges

The drag, added mass, shear lift, Magnus lift, and Basset history forces have been formulated as previously published in the literature. The drag force, as defined here, is valid for the entire range of Reynolds numbers encountered. The form of the shear lift force was originally verified for turbulent flow. Also, theoretically a solid sphere in an inviscid fluid has an added mass coefficient value of 0.5; so, the added mass force defined herein is applicable to large Reynolds number flows, too. From Rubinow and Keller (1961), the Magnus force was derived for low Reynolds number flows only. The Basset history force is not well known for low Reynolds number flow (Nino and Garcia, 1992). For analysis purposes, the forces are extended to the entire range of Reynolds numbers. This follows the previous research procedures as done by Wiberg and Smith (1985) and Nino and Garcia (1992) which have yielded satisfactory results.

Equation of Motion

The equation of motion for a saltating particle may be divided into longitudinal and vertical components. The forces acting on a saltating particle are described by the following equations for a steady, horizontal flow.

$$\rho_s V\frac{du}{dt} = -C_D A\frac{1}{2}\rho\sqrt{\left(u-u_f\right)^2+w^2}\left(u-u_f\right) - \rho V C_M\frac{du}{dt} - \frac{6\pi\mu\left(\frac{d}{2}\right)^2}{\sqrt{\pi\upsilon}}\int_0^{T_s}\frac{\frac{du}{dt}}{\sqrt{T_s-\tau}}d\tau$$
$$+\frac{\pi}{8}d^3\rho\sqrt{\left(u-u_f\right)^2+w^2}\left(\Omega-\frac{1}{2}\frac{du_f}{dz}\right)\frac{w}{\sqrt{\left(u-u_f\right)^2+w^2}} + \rho(s-1)gV\sin\beta \tag{9}$$

and

$$\rho_s V\frac{dw}{dt} = -C_D A\frac{1}{2}\rho\sqrt{\left(u-u_f\right)^2+w^2}\left(w\right) - \rho V C_M\frac{dw}{dt} - \frac{6\pi\mu\left(\frac{d}{2}\right)^2}{\sqrt{\pi\upsilon}}\int_0^{T_s}\frac{\frac{dw}{dt}}{\sqrt{T_s-\tau}}d\tau$$
$$-\frac{\pi}{8}d^3\rho\sqrt{\left(u-u_f\right)^2+w^2}\left(\Omega-\frac{1}{2}\frac{du_f}{dz}\right)\frac{u-u_f}{\sqrt{\left(u-u_f\right)^2+w^2}} \tag{10}$$
$$+\frac{\rho}{2}AC_L\left(u_{\Delta Top}^2-u_{\Delta Bot}^2\right)-\rho(s-1)gV\cos\beta$$

where

$$u_{\Delta Top}^2 = \left(u-u_{fTop}\right)^2+w^2 \tag{11}$$

and

$$u_{\Delta Bot}^2 = \left(u-u_{fBot}\right)^2+w^2 \tag{12}$$

The variables, u_{fTop} and u_{fBot}, are the fluid velocities evaluated at the top and bottom of the particle, respectively. The quantities, u and w, are the particle's translational speed parallel and normal to the bed, respectively. All these assume no w-component of fluid velocity. Figure 1 provides a sketch of the particle forces. β is the bed slope as defined in Figure 2.

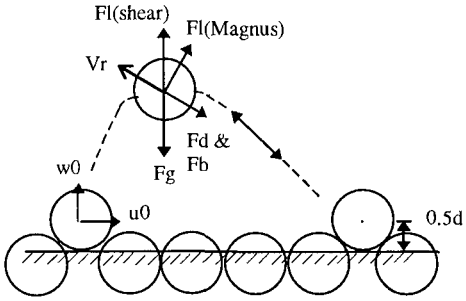

Figure 1 Force definition sketch of particle saltation

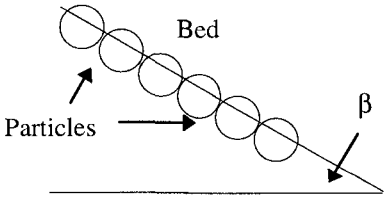

Figure 2 Definition of bed slope

The fluid velocity profile used in the model is the "law of the wall" profile,

$$\frac{\bar{u}}{u_*} = \frac{1}{\kappa}\ln\left(\frac{29.7z}{k_s}+1\right) \tag{13}$$

where $\bar{u}$ is the mean fluid velocity, u_* is the fluid friction velocity, κ is Karman's constant, z is height above the "theoretical bed", and k_s is the bed roughness. The "theoretical bed" is located at z = 0. Note that the fluid velocity has only a horizontal, or bed-parallel, component.

Boundary Conditions

The "theoretical bed" is assumed to be 0.2 times the particle diameter below the top of the particles as is shown in Figure 3. The initial position of the saltating particle is at one-half a particle diameter above the "theoretical bed". In order to solve the equations of motion given previously, the particle's initial vertical and horizontal velocity components are needed. The values of these components come

from the equations of White and Schulz (1977). They found that the speeds varied from u_* to $2u_*$. In addition, they found that lift-off angles varied from 30 to 70 degrees. When the Magnus force is considered, an initial particle angular velocity is needed. This value is adjusted to yield a best match to a known trajectory.

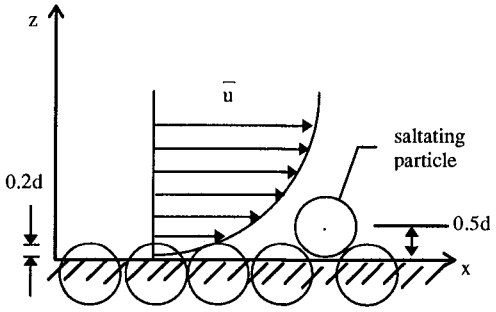

Figure 3 Saltating particle initial position

Method of Solution

The equations of motion along with the moment equation are defined as first order ordinary differential equations. A fourth order Runge Kutta approach is used to yield a vertical and horizontal particle velocity and an angular velocity. The vertical and horizontal velocity components are numerically integrated with a simple Simpson's Rule approach to obtain a particle trajectory. The model includes some adjustable parameters. The bed roughness can be taken to be any multiple of the particle diameter. The initial velocities, angular velocity and the lift-off angle also may be adjusted.

Sensitivity Analysis

This section looks at the relative effect force combinations and initial conditions have in determining the trajectory of a saltating grain. The parameters that are held constant unless otherwise specified through the force sensitivity test are grain diameter, specific gravity, initial particle velocity, initial angle, and bed roughness. They are 0.18 cm, 2.65, $2u_*$, 45 degrees, and 2d, respectively. The coefficient of lift was taken to be 85% of the coefficient of drag. These are the values that were either used or observed by Fernandez Luque and van Beek (1976). In addition, it needs to be stated that the bed slope was taken to be zero in this case.

The most basic form of the model contains the drag, added mass, and gravity forces. The shear lift force developed by Wiberg and Smith (1985) and the history force from Basset (1888) are successively added to the model. Figure 4 shows the results. For this case, $u_* = 4$ cm/s with $u_0 = w_0 = 2u_*$. The shear lift force increases the length of the trajectory by about one grain diameter while the Basset history

force appears to have a lesser effect on the trajectory. The results with the shear lift force included are consistent with our intuition. Only a small velocity gradient develops across the grain because of its size. As a result, the shear lift has a relatively small effect. The height is increased by less than one-tenth of a grain diameter while the length increased by approximately one-half grain diameter when the Basset term is included. The increase in length is due to the fact that the grain travels higher into the fluid column and thus attains a greater velocity.

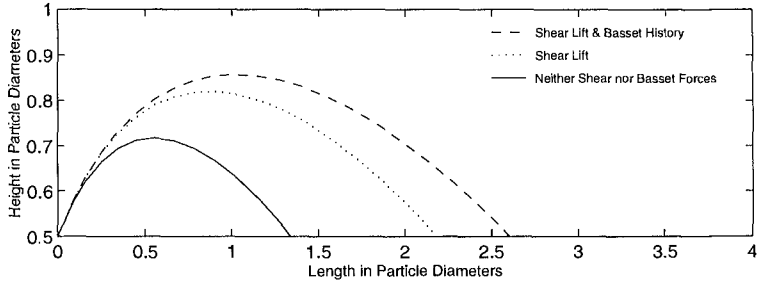

Figure 4 Effect of shear lift and Basset history forces on small particle

We then ran the model with a larger particle size. A diameter of 3.1 cm was chosen, roughly in the gravel regime. The other parameters maintained their same values with the exception of $u_* = 22.84$ cm/s and $\beta = 0.07$ to match the experimental conditions of Nino et al. (1992). Figure 5 shows that the shear lift force had more of an effect than it did with the smaller grain. This result is expected because the velocity gradient is large on a larger particle. The Basset force, however, did not posses the same significance as it did in the other case. This force had little effect on the particle trajectory. The Basset history force had a greater effect on the smaller particle than on the larger particle. This same result was obtained by Nino and Garcia (1992).

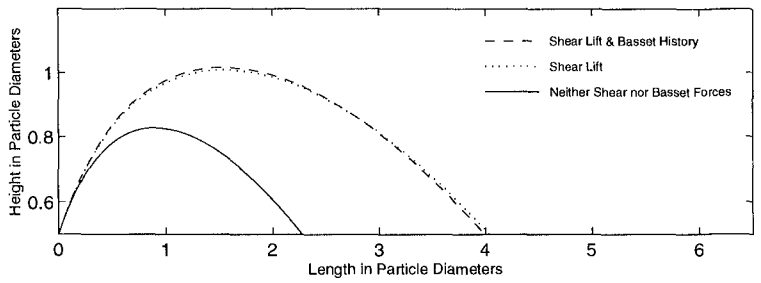

Figure 5 Effect of shear lift and Basset history force on a large particle

The next force to consider adding to the formulation is the Magnus lift force. To review, this force results from grain rotation which is caused in two ways. First, a grain may be transferred an angular velocity from the shear flow. Since the fluid velocity is greater at the top of a grain than at the bottom of a grain, a net torque may

be exerted upon the grain. Second, a grain on the bed may obtain an angular velocity from a collision with another grain. The magnitude of the rotation is dependent on the speed and the placement of the blow that the grain striking the bed delivers. Figure 6 displays the trajectories that result by varying the initial angular velocity. The diameter of the particle is 0.18 cm with k_s=2d, C_L=0.85C_D, u_*=4 cm/s, u_0=2u_*, and w_0=2u_*. It is obvious and expected that the trajectories should both increase in length and height with increasing initial angular velocity. The effect of the Magnus force on a particle's path is quite significant. This is a somewhat discouraging result because little is known about the angular velocities of saltating grains. A common practice is to match a known trajectory by "tweaking" the initial angular velocity of the particle.

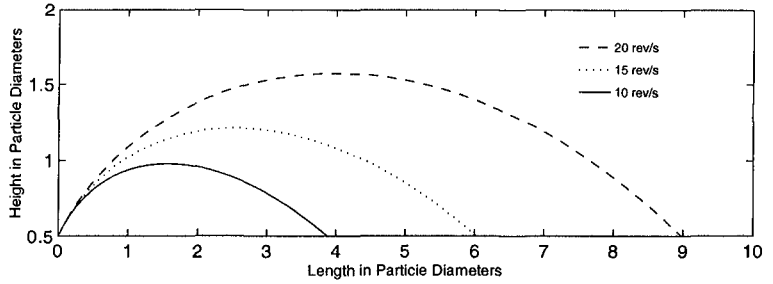

Figure 6 Effect of Magnus force on particle trajectories

The initial angle and velocity of the grain is the next area of interest. Again the grain size used is 0.18 cm. Figure 7 displays the results of varying the take-off angles and maintaining a constant initial velocity. The initial angles are 30, 45, and 60 degrees. The initial longitudinal velocity and initial vertical velocity are both 2u_*. Figure 8 shows what happens if the velocities are varied and the angles are held constant at 45 degrees. As the lift-off angles increased, the grains saltated farther. Also, the higher the initial velocity, the longer the trajectory. These results are obviously from the fact that the grain attains a higher velocity from the fluid with a larger angle and higher initial velocity.

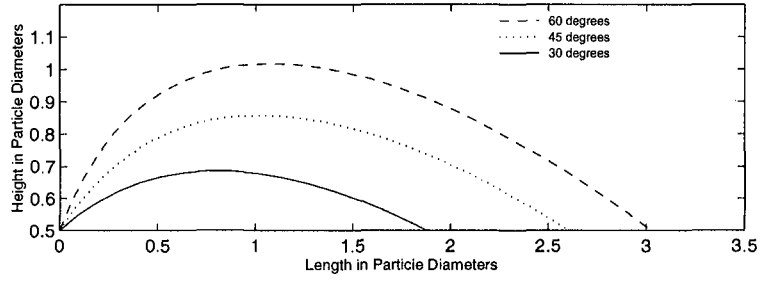

Figure 7 Trajectory sensitivity to particle take-off angle

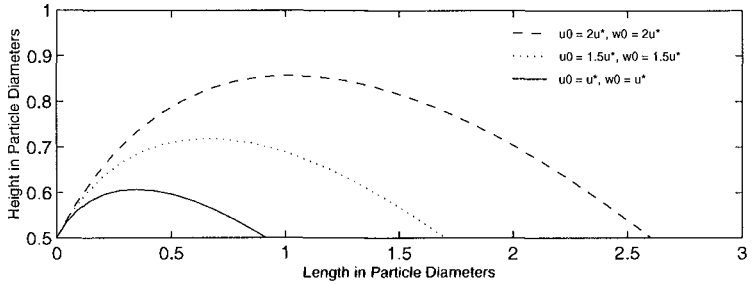

Figure 8 Trajectory sensitivity to particle take-off speed

To summarize, the forces acting on the particle vary significantly with grain size. The shear lift force and the Basset history force vary the greatest of the forces examined. The Magnus effect increases saltation length and height greatly as initial angular particle velocity increases. Finally, the larger the initial velocity and angle, the greater the saltation length and height.

Comparison of Model to Data

The Magnus Effect is neglected for the first comparison with a given data set to see if the shear lift force is sufficient. The trajectory data used for the model comparison is provided by Fernandez Luque and van Beek (1976). The grain diameter was 0.18 cm with a friction velocity of 4 cm/s. The initial conditions for the model were u_0 = 8 cm/s, w_0 = 8 cm/s, β = 0, $C_L = 0.85C_D$, and k_s = 2d. The trajectory is shown as the solid line in Figure 9. It is easily seen that the shear lift force alone does not adequately describe the motion of the particle as observed by Fernandez Luque and van Beek (1976).

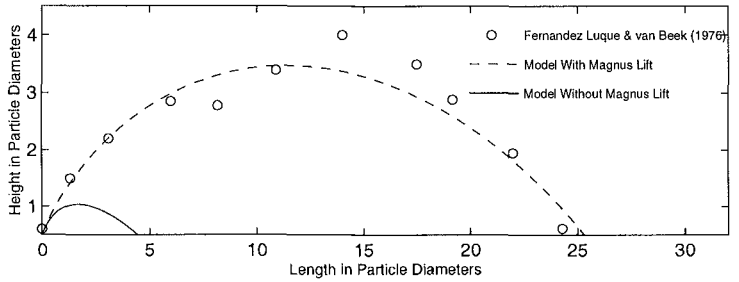

Figure 9 Model comparison to Fernandez Luque and van Beek (1976) observations

Figures 10 through 14 show some of the relevant velocities and forces as predicted by the model. The fluid velocity is always in the rough, turbulent range as shown by the Reynolds number. The drag coefficient was between 0.60 and 0.85. Those quantities are graphically shown in Figure 10 and Figure 11. Figure 12 shows how the particle, fluid, and relative velocities varied over the trajectory length of the saltation. The plot reveals that the particle velocity is continuously increasing

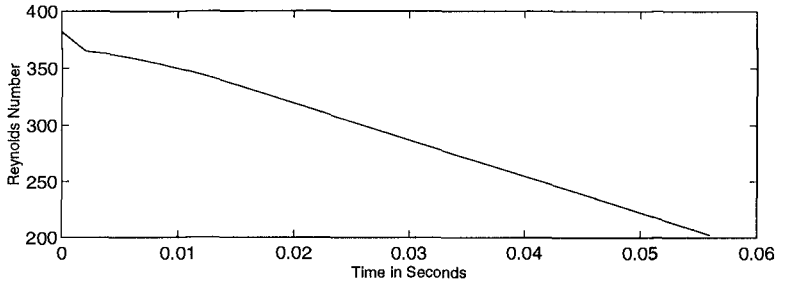

Figure 10 Reynolds number simulated saltation trajectory

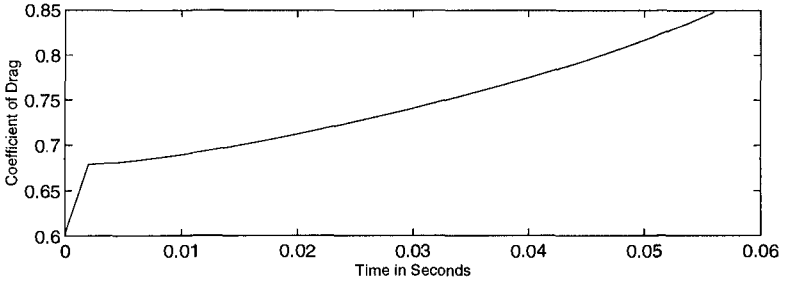

Figure 11 Drag coefficient for simulated saltation trajectory

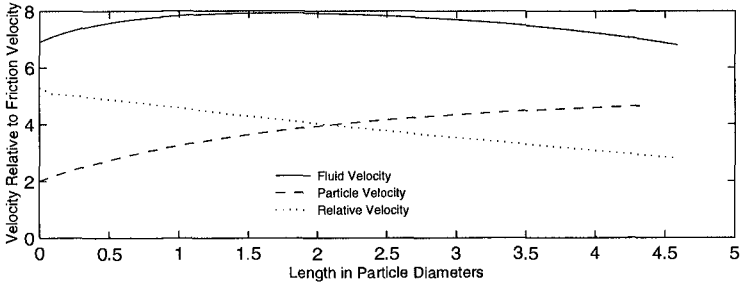

Figure 12 Strength of velocities of simulated particle trajectory

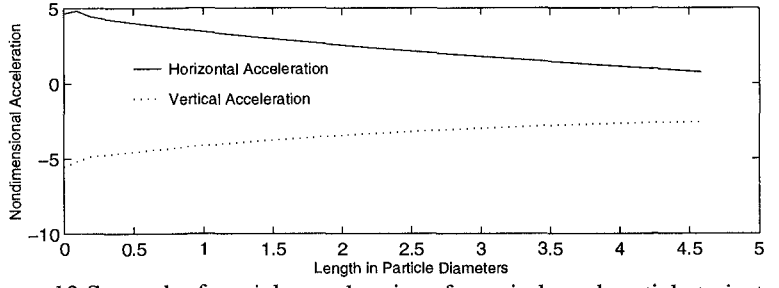

Figure 13 Strength of particle accelerations for a simluated particle trajectory

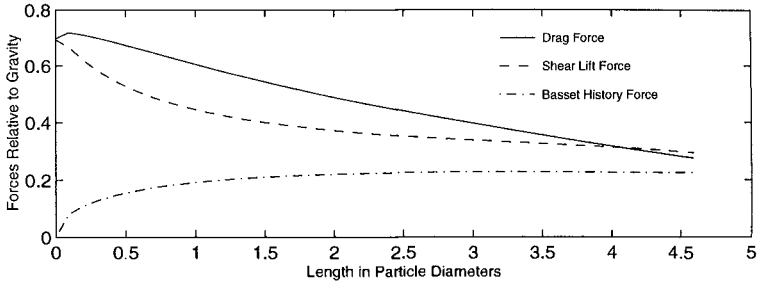

Figure 14 Strength of relevant forces for a simulated particle trajectory

toward that of the fluid velocity. So as a result, the relative velocity is decreasing. This means that the drag and lift forces are both decreasing over the grain trajectory. This is shown in Figure 14. The drag force is represented by the solid line and the shear lift force is represented with a dashed line. The Basset history force is smaller than both the lift force and the drag force for much of the saltation also in Figure 14. These forces in this figure are given relative to gravity. Note that the Basset force continually increases as the particle saltated as a result of the integral nature of the force.

The horizontal acceleration of the particle decreases as the particle velocity approaches the fluid velocity as shown in Figure 13. The vertical acceleration becomes less negative as the particle saltates. The accelerations are non-dimensionalized by multiplying the acceleration by T_s/u_*. The particle decelerates significantly in the rising part of the trajectory and continues to do so until the particle approaches the bed. It accelerates again near the bed because of the aforementioned lift force. This shear lift force is significant when compared to the drag force. It is evident from Figure 9 that the lift force is not providing enough upward thrust for the particle to saltate as observed by Fernandez Luque and van Beek (1976).

The Magnus force was added to the equation of motion to improve the agreement with observations. In addition, the moment equation was added and solved simultaneously with the equation of motion. The initial conditions were maintained with one exception. An initial angular velocity, Ω_0, of 30 rev/s was added. The model comparison with the data range is displayed in Figure 9. The model now predicts the grain trajectory fairly well and certainly much better than previously. The Magnus force significantly increases the overall lift effect on the particle especially in the rising part of the trajectory according to Figure 15. For this particular case, the Magnus force increased the saltation height by 2.3 grain diameters and the length by 21 grain diameters. Wiberg and Smith (1985) reached a similar conclusion that the Magnus force should be included.

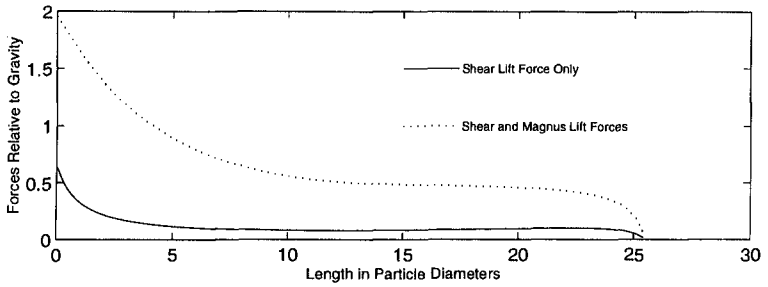

Figure 15 Comparison of shear lift and Magnus forces

Conclusion

The saltation model considered particles from incipient motion through a trajectory and returning to the bed. The saltation model included gravity, added mass, drag, shear lift, Magnus lift, and Basset history forces. The shear lift force is the same as defined by Wiberg and Smith (1985). When the Magnus lift force is applied, the moment equation from White and Schulz (1977) is used to continually update the particle's rotation.

It was found that a particle will saltate farther with increasing take-off speed and angle. The shear lift and Basset history forces vary significantly with particle size. The shear lift force has a greater effect on large particles and Basset history has a greater effect on small particles. The Magnus lift force affects trajectories significantly when included in the model formulation.

The model is able to match observed trajectories from Fernandez Luque and van Beek (1976). It is necessary to include the Magnus lift force to best match their observations. The shear lift force may need further examination. It appears to underpredict the velocity gradient that is expected at the end of a particle's trajectory near bed. These results suggest experiments be conducted to measure the rotation of saltating grains.

Acknowledgments

This work was supported by the U.S. Office of Naval Research, Coastal Sciences Program. Discussions with Renwei Mei are appreciated.

References

Auton, T.R., Hunt, Jc.R., and Prud'Homme, M., The force exerted on a body in inviscid unsteady nonuniform rotational flow, J.Fluid Mech., 197, 241-257, 1988.

Abbott, J. E., and Francis, J. R. D., Saltation and suspension trajectories of solid grains in a water stream, Phil. Trans. R. Soc. London, Ser. A, 284, 225-254, 1977.

Bagnold, R. A., The nature of saltation and of 'bed-load' transport in water, Proc. R. Soc. London, Ser A, 332, 473-504, 1973.

Basset, A. B., A Treatise on Hydrodynamics Volume Two, Dover Publications, New York, 1888.

Chepil, W. S., The use of evenly spaced hemispheres to evaluate aerodynamic forces on a soil surface, Trans. AGU, 39 (3), 397-404, 1958.

Einstein, H. A., The bed-load function for sediment transportation in open channel flow, U.S. Dept. Agric., Tech. Bull. no. 1026, 1950.

Fernandez Luque, R., and van Beek, R., Erosion and transport of bed-load sediment, J. Hydraulic Res., 14 (2), 127-144, 1976.

Gilbert, G. K., Transportation of debris by running water, U. S. Geol. Survey Prof. Paper, 86, 1914.

Graf, W.H., Hydraulics of Sediment Transport, Water Resources Publications, Littleton, Colorado, 1984.

Krecic, M. R., Evaluation and development of particle saltation Models, thesis presented to the University of Florida, Gainesville, Fl, in 1995, in partial fulfillment of the requirements for the degree of Master of Science.

Lee, H. Y., and Hsu, I. S., Investigation of saltating particle motions, J. Hydr. Engrg., 120 (7), 831-845, 1994.

Mei, R., Flow due to an oscillating sphere and an expression for unsteady drag on the sphere at finite Reynolds number, J. Fluid Mech., 270, 133-174, 1994.

Morsi, S. A., and Alexander, A. J., An investigation of particle trajectories in two-phase flow systems, J. Fluid Mech., 1972 (part 2), 193-208, 1972.

Murphy, P. J., and Hooshiari, H., Saltation in water dynamics, J. Hydr. Div., ASCE, 108 (HY11), 1251-1267, 1982.

Nino, Y., and Garcia, M., Gravel saltation 2. modeling, Water Resour. Res., 30 (6), 1915-1924, 1994.

Nino, Y., M. Garcia, and L. Ayala, Gravel Saltation 1. Experiments, Water Resour. Res., 30 (6), 1907-1914, 1994.

Owen, P. R., Saltation of uniform grains in air, J.Fl. Mech., 20(Pt 2), 225-242, 1964.

Patel, M. H., Dynamics of Offshore Structures, Butterworth & Co. Ltd, NY, 1989.

Rubinow, S. I., and Keller, J. B., The transverse force on a spinning sphere moving in a viscous fluid, J. Fluid Mech., 447-459, 1961.

Van Rijn, L. C., Sediment transport, Part I: Bed load transport, J. Hydr. Engrg., 110 (10), 1431-1456, 1984.

White, B. R., and Schulz, J. C., Magnus effect in saltation, J. Fluid Mech., 81 (part 3), 497-512, 1977.

Wiberg, P. L., and Smith, A theoretical model for saltating grains in water, J. Geophys. Res., 90, 7341-7354, 1985.